Original Article

Effectiveness of Nanoclay in Stabilising Recycled High-Density Polyethene Modified Bituminous Mix

Zakaria Mohamed Barrie[1], Timothy Nyomboi[2], Kiplagat Chelelgo[3]

[1,2]*Department of Civil Engineering, Pan African University Institute for Basic Sciences, Technology, and Innovation (PAUSTI), Nairobi, Kenya.*
[3]*Department of Civil Engineering, Dedan Kimathi University of Technology, Nyeri, Kenya.*

[1]*Corresponding Author : zakariamohamedbarrie@gmail.com*

Abstract - In recent years, increased traffic volume and severe environmental conditions have increased the requirement for improved performance in bituminous pavements. High-Density Polyethylene (HDPE) is one of the most commonly used Polyethylene. HDPE improves bituminous pavement's high-temperature performance. However, HDPE-modified binder has been observed to be associated with phase separation and poor workability, limiting its widespread application. Recently, nanomaterials have been used to balance the undesirable effects of polymers while enhancing the bituminous binder and mixture performance. Hence, the research aims at producing a stabilised and workable HDPE-modified binder using nanoclay. HDPE content of 2%, 4%, 6%, and 8% was used to modify the 80/100 base binder. Nanoclay content of 1%, 2%, 3%, and 4% was used to stabilise the optimum HDPE-modified bitumen binder. The binders were tested using penetration, storage stability, ductility, softening point, and dynamic shear rheometer tests, while the bituminous mixtures were evaluated using volumetric and Marshall properties. Furthermore, microstructural tests were used to investigate the physical and chemical interactions between the additives and binders. Compared to the Kenya Roads Design Manual for Roads and Bridges Part III (RDMIII) specifications, the optimal dosage of HDPE was 4%, resulting in the highest Marshall stability of 13.9kN, lowest air voids of 4.9%, and 65.1% voids filled with binder, meeting all specifications. Additionally, adding 3% nanoclay to the optimal HDPE-modified binder showed superior performance, reducing viscosity by 47.8% and air voids by 12.3% while increasing Marshall stability by 30.2% and enhancing storage stability by 82.4% compared to the optimal HDPE-modified bituminous mix.

Keywords - Bituminous binder modification, High-density polyethylene, Microstructural properties of modified binder, Nanoclay, Storage stability.

1. Introduction

Bitumen is a well-known black, viscous, and hydrophobic engineering material whose physical and rheological properties vary significantly with time and temperature [1,2]. Its cohesive and adhesive properties make it suitable for paving applications. The paving industry requires a bitumen binder with flexibility, resistance against rutting, and thermal cracking resistance. Most conventional bitumen on the market does not offer all the necessary properties at once. As a result, they show limited resistance to rutting when exposed to high temperatures and high traffic [3]. They become brittle at low temperatures and thus cannot withstand the stresses induced by the loads, resulting in crack formation [4]. Hence, there is a need to modify conventional bituminous binders. The commonly and most widely used modifiers are polymers, chemical modifiers, anti-stripping additives, stiffening agents, extenders, oxidants, and antioxidants.

Polymer-modified bituminous binders have gained emerging interest in the paving industry due to their outstanding performance in terms of stiffness, resistance against rutting, resistance against thermal cracking, fatigue resistance, durability, and resistance to moisture damage [3,5]. Polymers like ethylene-vinyl acetate, styrene-butadiene-styrene, polyethylene, styrene-butadiene rubber, ethylene butyl acetate, polybutadiene, styrene-ethylene-butadiene-styrene, polypropylene, polyvinyl chloride, and polystyrene are used in bitumen binder modification. Polyethylene is a popular and suitable polymer due to its low melting point, resistance to deformation, cost-effectiveness, and homogeneous mixing with bitumen [6]. When used in bitumen modification, their mixing temperature ranges from 150°C to 180 °C, with a percentage dosage of 1% to 10% [7]. Polyethylene is a versatile material with various types, including linear low-density (LLDPE), high-density (HDPE), medium-density (MDPE), and low-density (LDPE). HDPE has emerged as a widely employed polyethylene in modifying bitumen owing to its capacity to enhance resistance against rutting and sensitivity to temperature changes [8,9].

Nevertheless, HDPE-modified bitumen binders exhibit high storage instability due to density variations, oxidation, poor bonding between the binder and polymer [6] and poor workability due to high viscosity [10]. Poor stability will

compromise the homogeneity and consistency, and poor workability will make it challenging to handle, transport, and apply during the construction of the HDPE-modified binder. This limitation can result in difficulties in achieving uniform coverage, proper compaction, and desired pavement quality, leading to potential performance issues and reduced durability. Therefore, an attempt to address these limitations is to incorporate complementary additives that can balance the undesirable impact of HDPE while improving the bituminous binder and mix performance.

Nanomaterials such as carbon nanotubes, nanoclay, graphene and its oxidants and nanosilica are used in polymer-modified bitumen to enhance storage stability and performance, particularly at high temperatures [11,12]. Among them, nanoclay has gained attention for improving polymer-modified bitumen's storage stability and phase separation [12,13], improved workability [14] and is safe, cheap, and long-lasting [15]. Recent studies have demonstrated that adding nanoclay to the bitumen binder lowers the viscosity, making mixing and handling at lower temperatures much simpler than unmodified bitumen binder [14, 16]. [14] observed that nanoclay in bitumen reduces the unmodified bitumen's penetration and increased softening point.

Furthermore, [15] observed a softening point difference of less than 2.5°C when 2% and 3% nanoclay was added to the SBR-modified binder, indicating improved compatibility. A remarkable enhancement of storage stability was also observed when nanoclay was incorporated into SBS-modified and crumb rubber-modified binders [13, 17]. In their study, [18] observed a significant improvement in bitumen rutting resistance when nanoclay was added. The interaction mechanism of the nanoclay with the bitumen supports these improvements. During stabilisation, the polymer chains are entrenched in the clay interlayer, causing silicate particles to disperse and penetrate the polymer matrix. As a result, the polymer expands to allow for polymer intercalation or exfoliation between the unit layers, resulting in a polymer-clay nanocomposite.

Although earlier studies have looked at high-density polyethylene (HDPE) as a modifier, most focus on pure HDPE, which is expensive compared to recycled HDPE. Moreover, most previous research has reported the effectiveness of nanoclay in improving SBR, SBS and crumb rubber-modified bitumen storage stability [13, 15, 17]. However, limited literature has explored the stabilisation of recycled HDPE using nanoclay.

Hence, there is a gap in investigating the effectiveness of nanoclay in stabilising recycled HDPE-modified binders. Therefore, this study endeavoured to use recycled HDPE to modify bitumen binder and nanoclay to stabilise HDPE-modified binder and thus evaluate the binder's physical, rutting and microstructural properties and their mixture's Marshall and volumetric properties.

2. Materials and Methods
2.1. Bitumen
This research used conventional 80/100 penetration grade bitumen to produce the modified bitumen. The selection of this bitumen was based on its predominant use in regions with high temperatures, where the bitumen must resist softening and deformation due to heat. Jilk Construction Company in Kenya supplied this bitumen. The bitumen was characterised using a softening point following ASTM D36 [19], ductility as per ASTM D113 [20], specific gravity, penetration following ASTM D5 [21], and rotational viscosity in accordance with AASHTO T316 [22]. The binder's physical properties are shown in Table 1.

2.2. Aggregates
The granite aggregates used were sourced from a HYoung Company Quarry in Kenya. Double-crush aggregates were selected to mitigate the flakiness and elongation challenges during compaction and enhance a stable skeleton with good interlocking effects. The aggregates' gradation was based on the Kenya Design Manual for Roads and Bridges Part III (RDMIII) for producing 0/20mm Asphalt concrete (AC) Type I binder course.

This AC type I was selected to design for heavy traffic of ≥ 25 million equivalent single axle loads (MESALs). The maximum nominal size of this gradation was 19.0 mm. Sieve analysis was performed on 14/20mm, 10/14mm, 6/10mm and 0/6mm samples, and their combined overall gradation is shown in Figure 1. The aggregates' physical and mechanical properties are presented in Table 2.

2.3 High-Density Polyethylene
This study utilised recycled high-density polyethene pellets purchased from Mr Green Africa Trading, a recycling company in Kenya.

The supplier gave some physical properties, such as density, water absorption, humidity, melt flow rate, and melting point. Figure 2 shows an illustration of recycled HDPE pellets.

Table 1. Physical properties of 80/100 Bitumen

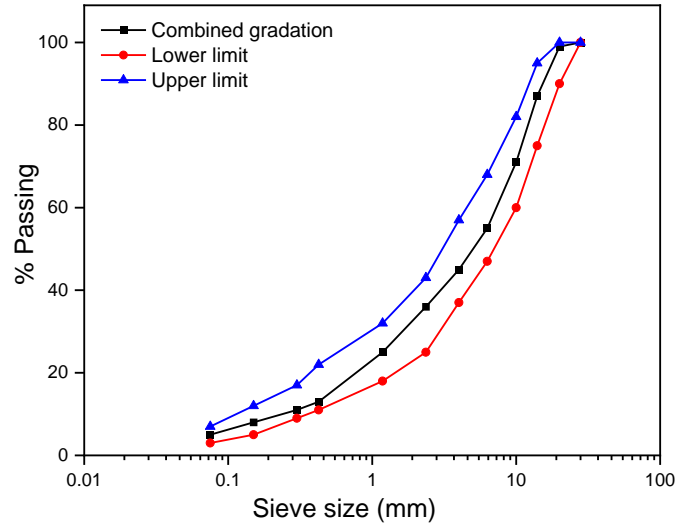| Test	Test standard	Result	Specifications (As per ASTM)
Penetration @ 25ºC	ASTM D5	82	80-100
Ductility @ 25ºC (cm)	ASTM D113	125	>100
Specific gravity (g/cm3)	ASTM D70	1.02	1.01-1.06
Rotational viscosity (cP @ 135ºC)	AASHTO T316	280	3000
Softening Point (ºC)	ASTM D2398	48	40

Fig. 1 Aggregates gradation for DBM type I binder course

Table 2. Physical and mechanical properties of aggregates

Test	Test standard	Value	Specifications (Kenya RDMIII)
Coarse Aggregates			
Los Angeles Abrasion (%)	ASTM C131-89	15	30 (max)
Aggregate Impact Value (%)	BS 812-112 (1990)	18	25 (max)
Elongation Index (%)	BS 112: Sec. 105.2 (1990)	14	20 (max)
Flakiness Index (%)	BS 112: Sec. 105.1 (1990)	14	20 (max)
Water Absorption (%)	ASTM C127	2.469	
Bulk specific gravity (Gsb)	ASTM C127	2.504	
Fine Aggregates			
Water Absorption (%)	ASTM C128	3.879	
Bulk Specific gravity	ASTM C128	2.452	
Filler			
Bulk Specific gravity	ASTM D854-02	2.559	
Total Bulk Sp. Gr (Gsb)		2.486	

Fig. 2 Recycled high-density polyethylene

2.4. Nanoclay

The study utilised high-purity organically modified montmorillonite (OMMT) nanoclay purchased from ULTRANANOTECH in India. According to the supplier, the OMMT nanoclay was produced by modifying the clay with Cetyltrimethyl Ammonium Bromide (CTAB) chemical. Samples were examined for chemical characteristics, morphology, and particle size using X-ray fluorescence (XRF) analysis, Energy Dispersive X-ray

Spectrometry (EDS), X-ray diffraction (XRD) analysis, and Scanning Electron Microscopy (SEM) analysis. Fig. **3** shows an illustration of nanoclay samples.

Fig. 3 Organically Modified Montmorillonite (OMMT) nanoclay

2.5. Experimental Design

Fig. **4** illustrates the experimental design for this study. It outlined the procedures used in producing the HDPE-nanoclay bituminous binder and mixture, along with various tests conducted to assess the performance of the bitumen binder and mixture.
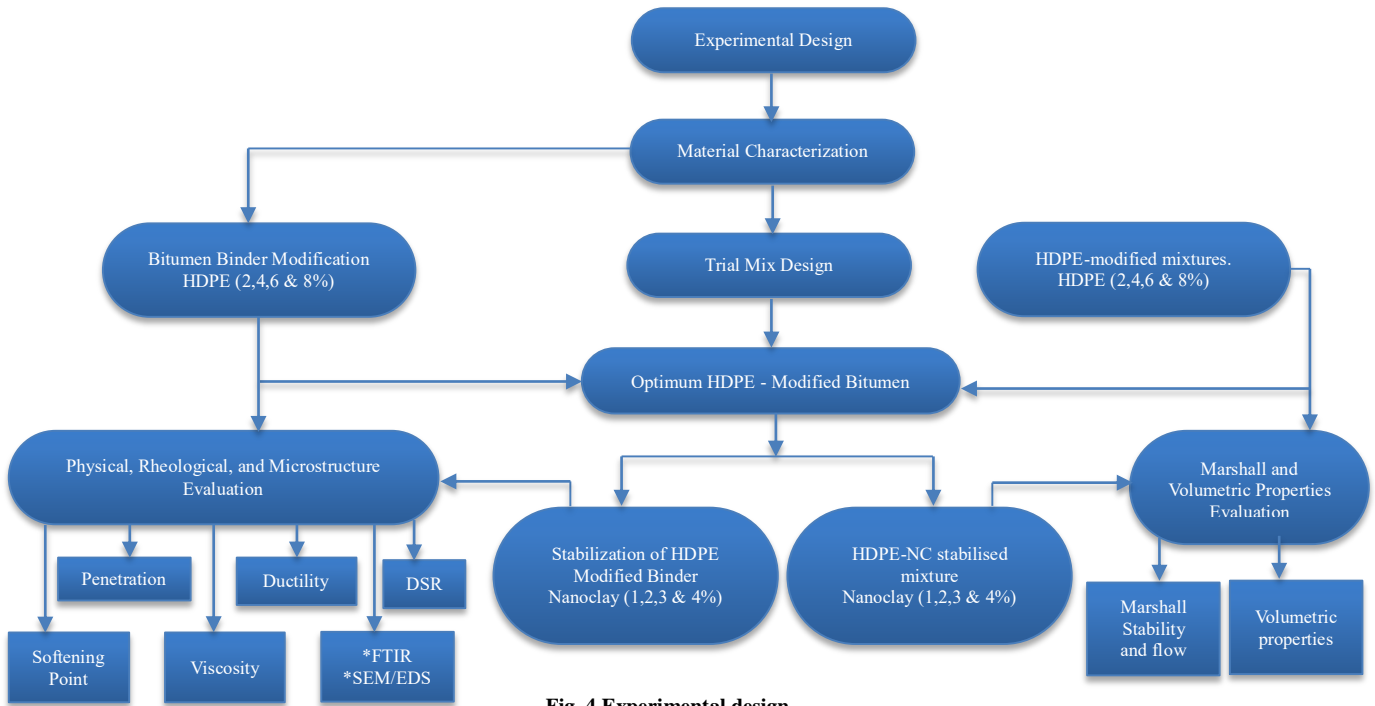
Fig. 4 Experimental design

2.6. Preparation of Modified Binder

The modified bitumen binders were prepared with HDPE and OMMT nanoclay using the wet-mixing method. The base binder was heated at 150℃ and stirred using a high-speed shear mixer at 4000 rpm for 10 minutes. This was done to eliminate any trapped moisture and air from the base binder. The high-speed shear mixer has a rotational speed ranging from 200 to 11000 rpm.

In preparing the HDPE-modified bitumen binder, 2%, 4%, 6%, and 8% HDPE by weight of the base binder was added to the base binder. These blends were mixed at $170 \pm 10℃$ at a constant stirring speed of 4000 rpm for 1 hour. After modification, all binders were set for 60 minutes at 180℃ in a static condition to allow proper interaction between the binder and the HDPE. The selected shear rate, mixing time and temperature were based on findings and reports from [8,23]. Moreover, the modified binders were evaluated using physical and rheological characterisation tests. Volumetric and Marshall properties of their mixtures were also evaluated to determine the optimal HDPE content. After evaluation, the optimum HDPE content was selected considering the specifications in the Kenya Road Design Manual for Roads and Bridges Part III.

For HDPE-nanoclay stabilised bitumen binder preparation, nanoclay with dosages of 1%, 2%, 3%, and 4% by weight of the base binder were utilised. The nano clay was added to the optimum HDPE-modified bitumen binder at $170 \pm 10℃$ at a constant stirring speed of 4000 rpm for 45min. Finally, these stabilised bitumen binders were set for 60 minutes at 180℃ in a static condition to allow proper interaction between the binder and the additives. The stabilised binders were assessed through physical, rheological, and microstructural analysis, along with volumetric and Marshall properties, to determine the nanoclay effect on the optimal HDPE-modified binder.

Moreover, the shear rate, duration, and temperature were adopted from a study by [12]. Fig. **5** illustrates the materials and equipment used during the modification process.
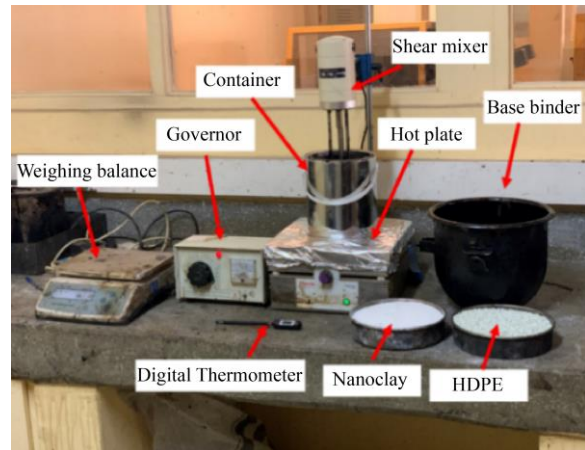

Fig. 5 Equipment and materials setup

2.7. Evaluation of Modified and Stabilised Bitumen Binders
2.7.1. Physical Characterisation

The main bitumen's physical characteristics tests, such as penetration in accordance with ASTM D5 [21], rotational viscosity as per AASHTO T316 [22], softening point following ASTM D36 [19], and ductility as per ASTM D113 [20], were carried out. The results of HDPE-nanoclay stabilised binders were compared with the optimum HDPE-modified binder and specifications from the Kenya RDMIII.

2.7.2. Rheological Properties Evaluation

In examining the unmodified, modified and stabilised bitumen binder resistance to rutting, the dynamic shear rheometer (DSR) test in line with AASHTO T315-10 [24] was conducted. This test focused on determining the shear

stress and linear viscoelastic properties of bitumen binder tested in oscillatory shear using parallel plates. The DSR rutting test consisted of a 25-mm parallel plate geometry and a 1-mm gap setting. The samples were short-term aged using a rolling thin film oven (RTFO). The ageing was done to simulate the impact of mixing and transporting the materials during pavement construction. The test aimed at measuring the rutting resistance factor ($G^*/\sin\delta$). This factor is measured from the complex shear modulus, known as the stiffness indicator G^*, and the phase angle (δ), known as the elasticity indicator. All tests were conducted using 10rad/sec single frequency and at temperatures of 64°C, 70°C, 76°C, 82°C, and 88°C.

2.7.3. Storage Stability of Modified and Stabilised Bitumen Binders

The storage stability test, in accordance with ASTM D7173 [25], evaluated the separation tendency of the binders during high-temperature storage. Modified and stabilised binders were heated, poured into aluminium tubes, and stored in an oven at 163°C for 48 hours. The tubes were then placed in a freezer for 4 hours at 10°C for cooling. After cooling, the tubes were divided into top, middle, and bottom parts, and softening point values for the top and bottom parts were documented. The difference in softening point values (SP_{diff}) between the top and bottom parts was used as the storage stability indicator.

2.7.4. Microstructural Properties of Bituminous Binders.

The microstructural characterisation test investigated the possible interactions among the bitumen binder, HDPE, and nanoclay. This was done using FTIR, SEM, and EDS. This preliminary evaluation was necessary since prior research has demonstrated that polymer-modified bitumen binders' final characteristics and stability depend on the type of local interactions and the relative miscibility of the components used. The FTIR analyses are used to identify the main organic compounds and chemical groups. The investigations utilised a wavenumber ranging from 4000 to 400 cm^{-1} using Bruker Alpha II FTIR instrument manufactured in Germany. SEM captured images using an acceleration voltage of 5 keV with a magnification of 5.00kx using Tescan MIRA SEM equipment. The EDS elementary analysis used Thermo Fisher Nove NanoSEM, Oxford X-Max detector, and INCA software. The FTIR samples were tested at Jomo Kenyatta University of Agriculture and Technology Juja, Nairobi, Kenya. SEM and EDX samples are tested at the Electron Microscope Unit, University of Cape Town, South Africa.

2.8. Bituminous Mixture Design and Preparation

The Marshall Mix design method as per ASTM D1559 [26] was used to estimate the optimal binder content for an Asphalt Concrete (AC) mixture. The mix design comprises aggregate sizes of 14/20mm, 10/14mm, 6/10mm and 0/6mm. The try-and-hit method procedure, as outlined in the Asphalt Institute's MS-2, 7th Edition 2014, was utilised to blend the aggregates to achieve a gradation that falls within the envelope specified by the lower and upper bounds of the Kenya RDMIII. Two series of Marshall specimens were fabricated. The first series of the specimens contained five binder contents: 4.0, 4.5, 5.0, 5.5, and 6.0% by weight of the mix. The second series was at the optimal bitumen binder content (4.8%) to evaluate the HMA volumetric and Marshall properties. The optimum binder content was determined as the mean binder contents that meet the maximum stability and 5.0% air voids. The determined optimum binder content was checked to see whether it had achieved the Kenya RDMIII specification limits of the five parameters: stability, flow, air voids, voids filled with binder and voids in mineral aggregate. The resulting optimum binder content was 4.8%. The final design mix comprised 15% 14/20mm aggregates, 19% 10/14mm aggregates, 21% 6/10mm aggregates, and 45% 0/6mm aggregates as a percentage by mass of the total dry aggregates with an optimum binder content of 4.8%.

2.9. Evaluation of Modified and Stabilised Bituminous Mixtures

2.9.1. Marshall Stability and Flow Test

This test evaluated the unmodified, modified and stabilised bituminous mixture predictive performance following ASTM D6927 [27]. In preparing the bituminous mixture, the optimum binder content (4.8%) obtained from the trial mixed design was used for both the HDPE-modified and HDPE-nanoclay stabilised bituminous mixtures. The use of the same binder content allowed for a more direct comparison of the effects of HDPE and HDPE-nanoclay on mixture properties than the conventional mix. In preparing the specimens, the binder and aggregates were combined and heated at 180 °C. The heated composite was placed in a cylindrical mode of 63.5mm height × 102mm diameter and compacted with 75 blows on both sides using a standard mould compactor.

2.9.2. Volumetric Properties

This study evaluated volumetric properties, including voids in the mix (VIM), voids in mineral aggregates (VMA), and voids filled with a binder (VFB). These are essential parameters for assessing the durability performance of bituminous mixtures. Maximum specific gravity (G_{mm}) and bulk density (G_{mb}) tests were used to determine the above volumetric parameters.

3. Results and Discussions

3.1. Physical Characterisation of Recycled High-Density Polyethylene

Table 3 shows that the HDPE sample has a density of 0.94 g/cm³, humidity content of 0.09%, melt flowability of 1.88 g/min, melting point of 132°C, water absorption of 0.05% and a diameter of 4.32 mm. The melting point shows that this plastic can be incorporated into bitumen without causing overheating of the binder during blending. Moreover, the sample exhibits good density, low water absorption, moderate melting point and melt flowability.

Table 2 reveals the physical and chemical compositions of nanoclay, with a dominant silicate (SiO_2) content of 75.69% and a high purity level of 99.5%. The silicon oxide highlights a layered silicate-type nanoclay that can disperse

and interact with polymer and bitumen phases. The high purity level of 99.5% is critical for ensuring that the nanoclay contributes positively to the modification process without introducing impurities. Its moderate specific gravity of 1.7 kg/m3 ensures even bitumen dispersion without compromising density.

Table 3. Physical properties of recycled high-density polyethylene

Test	Result
Physical State	Pellet
Colour	White
Density (g/cm3)	0.94
Humidity (%)	0.09
Diameter (mm)	4.32
Melting Flow Rate (g/min)	1.88/10
Water Absorption (%)	0.05
Melting Point (ºC)	132

3.2. Physical, Chemical and Morphological Characterisation of Nanoclay

Table 4. Physical and Chemical properties of nanoclay

Test	Result
Colour	White
Physical state	Powder
Purity (%)	99.5
Specific gravity g/cm3	1.7
XRD d001 (nm)	3.4
Chemical formula	$Al_2Si_2O_2(OH)_4$
Si_2O_2 (%)	75.69
Al_2O_3 (%)	11.44
CaO (%)	5.48
MgO (%)	4.10
K_2O (%)	2.33
P_2O_5	0.041
Others	0.919

Fig. **6** (a) and (b) present the images and elementary composition of nanoclay. The SEM images show the nanoclay plate layered structure with varying sizes. The layered structure indicated the presence of layered silicate, which is responsible for intercalating with the polymer during blending. The EDS micrograph reveals the presence

of oxygen (O), silicon (Si), Aluminium (Al), calcium (Ca), Potassium (K), Sodium (Na), Magnesium (Mg), and carbon (C). Since silicon dioxide (SiO_2) is the primary oxide of nanoclay, thus oxygen and silicon were expected. This result aligns with results from XRF and the SiO_2 unique phase present in the XRD results.

The result in the XRD spectrum in Fig. **6**c shows an intense diffraction peak at $2\theta = 19˚$, $2\theta = 27˚$, $2\theta = 29˚$, and $2\theta = 36˚$ with an interlayer spacing of 0.45mm, 0.33mm, 0.30mm, and 0.25mm, respectively. It was also observed that silicon dioxide (SiO_2) is the dominant mineralogy, making up 31%. Based on the crystallinity index and the average crystallinity size determined, it was observed that 70.9% of the nanoclay is made up of crystalline structure with an average size of about 25.8nm. Hence, the nanoclay is considered to be a nanocrystalline clay.

3.3. Evaluation of Optimum High-density Polyethylene Modified Bitumen Binder

The assessment of the optimum HDPE content considered the strength, workability and durability predictive parameters. These parameters were compared with Kenya Road Design Manual for Roads and Bridges Part III (RDMIII) specifications. Table 5 shows that 4% HDPE gave the highest Marshall stability and VFB and the lowest air voids compared to 2%, 6%, and 8% HDPE-modified mixture. The 4%HDPE-modified binder's viscosity, flow and VMA meet Kenya Road Design Manual Part III specifications. Hence, 4% HDPE content was adopted as the optimum due to its most satisfactory performance compared to Kenya Road Design Manual for Roads and Bridges Part III specifications. Moreover, 2, 6, and 8% HDPE do not meet at least one of the specifications as in the Kenya RDMIII.

3.4. Evaluation of High-density Polyethylene-Nanoclay Stabilised Binder
3.4.1. Physical Characterization
The nanoclay's effect on the HDPE-modified bitumen binder penetration, softening point value, rotational viscosity and ductility is depicted in Fig. **7** (a), (b), (c) and (d), respectively. It was observed that when the optimum HDPE-modified binder was dosed with 1%, 2%, 3%, and 4% nanoclay, the penetration improved by 25.1%, 42.6%, 70.3% and 65.6%, respectively.

Table 5. Summary of Optimum High-density polyethene modified bitumen binder

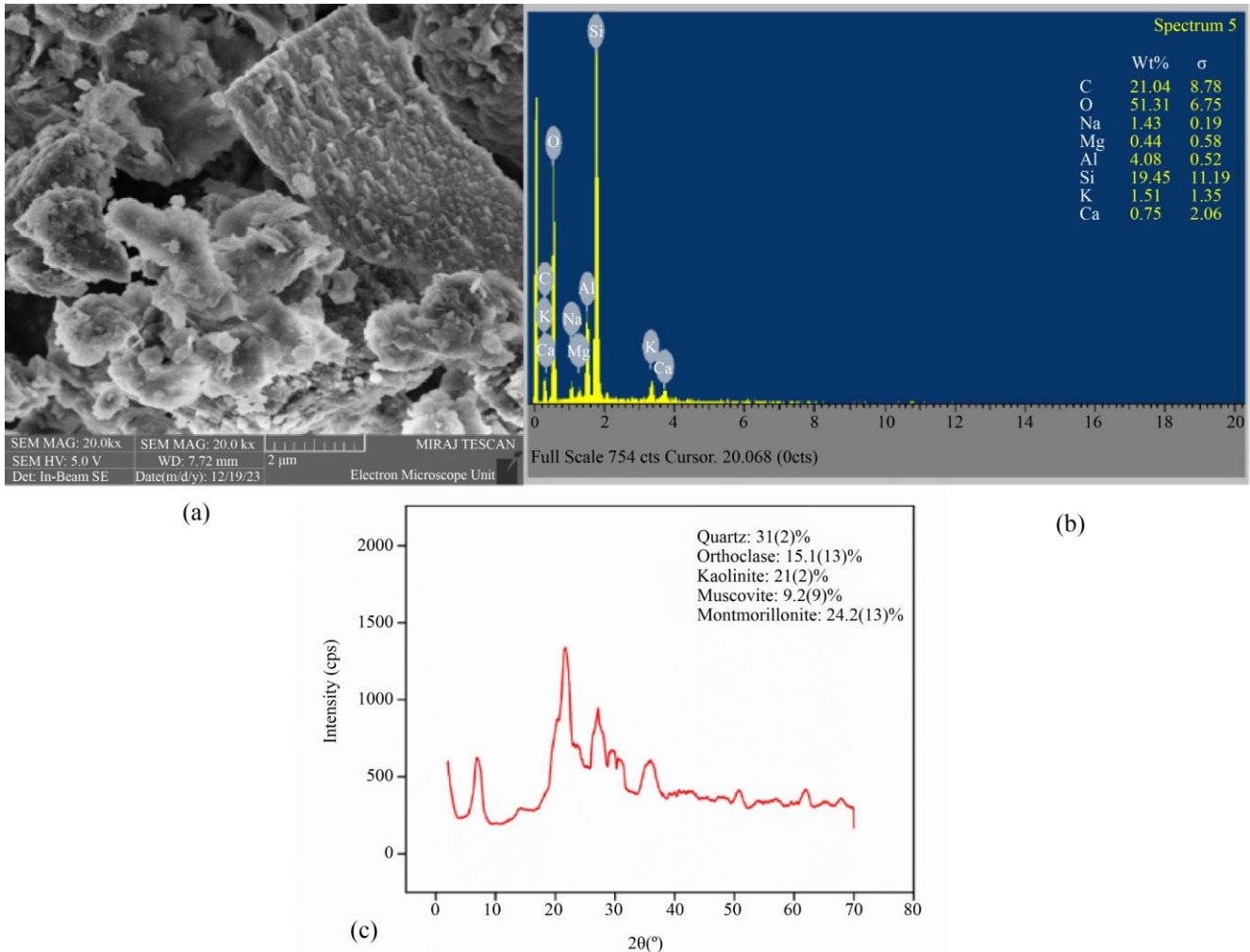| HDPE content (%)	Workability	Strength			Durability		
	Dynamic Viscosity ($\leq 3000cP$)	G*/sin(δ) 64°C ($\geq 2.2kPa$)	Stability (>9kN)	Flow (2-4mm)	Air voids (3-7%)	VMA ($\geq 14\%$)	VFB ($\geq 65\%$)
0	281	4.96	12.2	3.6	4.9	14.6	66.2
2	877	13.67	12.4	3.8	5.5	14.7	62.5
4	1972	22.36	13.9	3.9	4.9	14.1	65.1
6	3080	57.0	12.8	4.2	6.4	15.2	58.0
8	5970	195.08	11.9	4.0	7.1	16.0	55.2

Fig. 6 Microstructure properties of nanoclay (a) SEM micrograph, (b) EDS graph, AND (c) XRD plot.

In contrast, the softening point was reduced by 19.8%, 27.1%, 17.7% and 12.5%, respectively. Moreover, the viscosity reduced by 13.0%, 29.9%, 47.8%, and 27.7%, respectively, while the ductility increased by 3.6%, 7.1%, 8.9%, and 0.0%, respectively. An increased penetration, reduced softening point and lower viscosity indicate an enhanced cracking resistance performance at low temperatures. The reduced viscosity improves workability, lowering mixing and compaction temperatures during construction. This enhancement may be attributed to the effect of the Cetyltrimethyl Ammonium Bromide (CTAB) chemical during the clay's surface treatment process. Cetyltrimethyl Ammonium Bromide treatment contributes to a homogenous lubricating effect by increasing the basal spacing and reducing the particle agglomeration of the clay [28]. This phenomenon creates better dispersion during blending with the HDPE-modified binder. Moreover, an increased penetration, reduced softening point and lower viscosity with increased nanoclay content are attributed to the effective dispersion of the nanoclay, as shown in the SEM result in Fig. 12. This finding is consistent with findings from [14] and [16]. The reason for the unexpected enhancement in ductility remains unclear. It is noteworthy that a comparable increase in bitumen ductility was observed by [16] when nano-montmorillonite K10 was added to a base binder. According to the Kenya Design Manual for Roads and Bridges Part III specifications, all HDPE-nanoclay stabilised bitumen binder meets the criteria of viscosity $\leq$ 3000Cp.

3.4.2. Rheological Evaluation of High-Density Polyethylene-nanoclay Stabilised Binder

From the isochronal plot of HDPE-nanoclay stabilised binder in Fig. 8. It was observed that adding 1%, 2%, 3%, and 4% nanoclay increased the resistance against rutting (G*/sinδ) at all temperatures compared to a 4% HDPE-modified binder. The increase is linear, with 4%HDPE-4%nanoclay stabilised binder giving the highest value for all testing temperatures. This indicates that incorporating nanoclay increased the rutting factor, which increases the binder's resistance against rutting.

Moreover, it was also observed that the test temperature significantly influenced the rutting factor. Increased test temperature decreased resistance against rutting for all the HDPE-nanoclay stabilised binders. As compared to the AASHTO T321 specifications, the 4%HDPE-0%NC bitumen binder at 88°C does not meet the criteria of G*/sinδ > 2.2kPa, indicating that at a temperature of 88°C, the binder is prone to rutting failure.
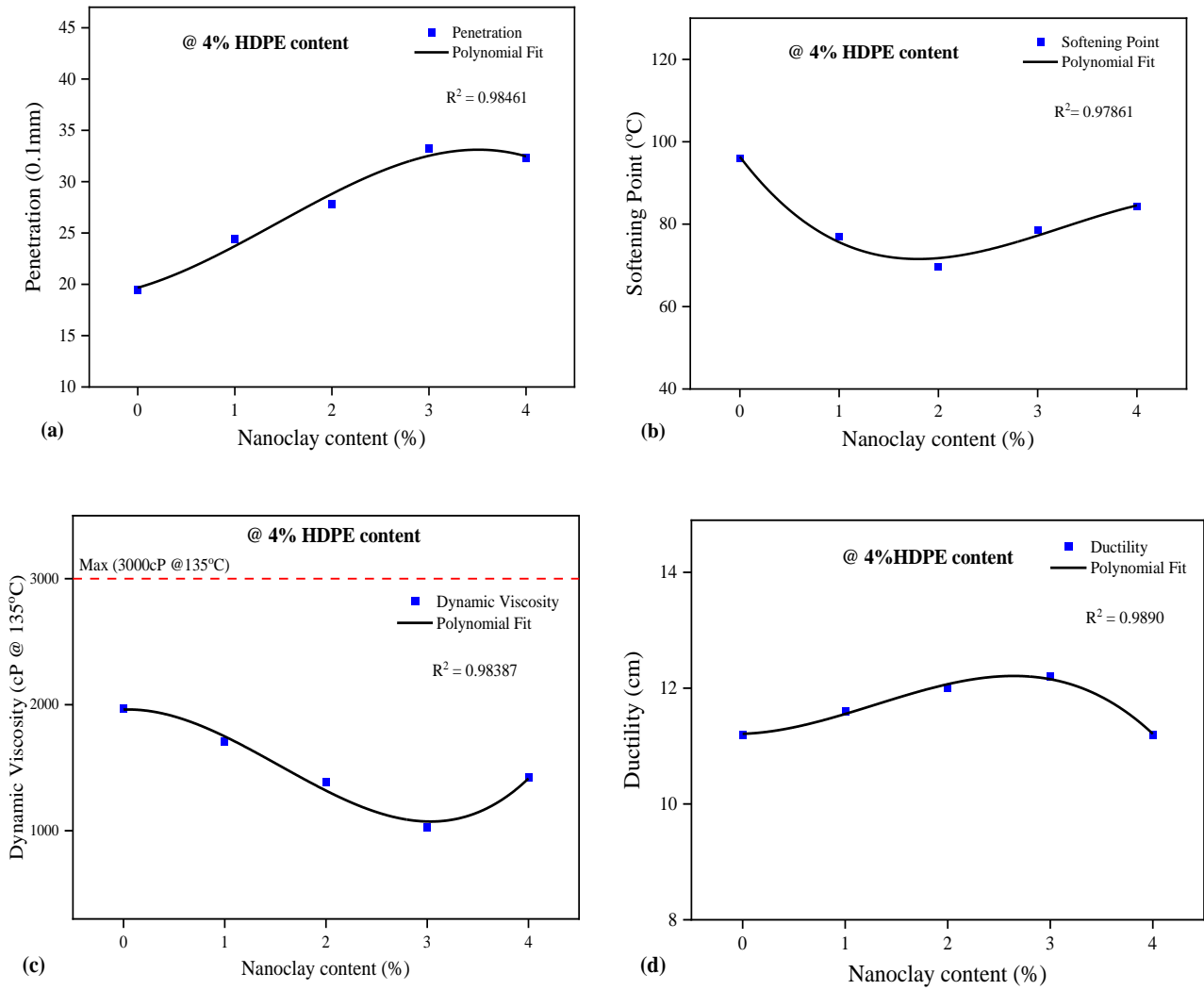
Fig. 7 Physical properties of HDPE-nanoclay stabilised binder (a) Penetration, (b) Softening point, (c) Dynamic viscosity, AND (d) Ductility.
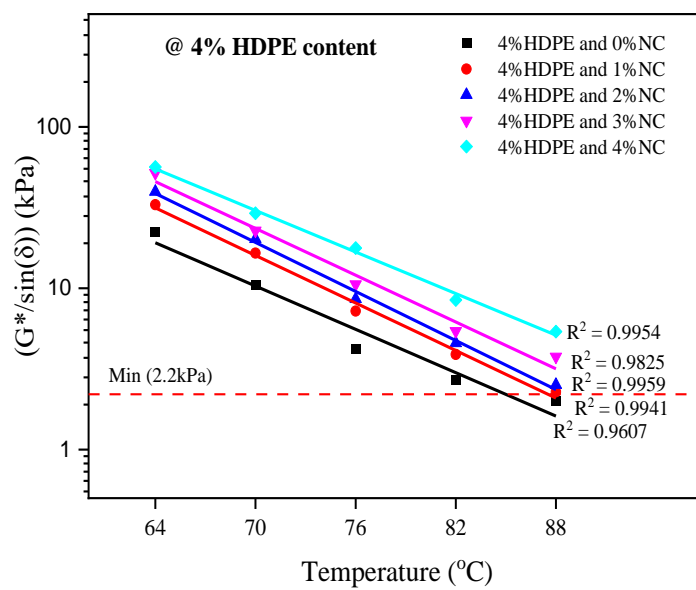

Fig. 8 Rheological properties of HDPE-nanoclay stabilised binder

3.4.3. Storage Stability Evaluation

Fig. **9** depicts the storage stability results for 4% HDPE-modified and HDPE-nanoclay stabilised binders. It was observed that increasing the nanoclay content caused a decrease in SP_{diff} values, indicating better compatibility at the storage level. A reduction of 6.2°C, 8.9°C, 10.9°C, and 11.3°C was observed when incorporating 1%, 2%, 3%, and 4% nanoclay in the HDP-modified binder. This finding might be attributed to the physical attraction between the clay and polymer networks. Penetration of nanoclay into the polymer network may have increased the settling velocity of the polymer due to their increased density compared to HDPE and bitumen binder, resulting in the dispersion of the polymer. Typically, polymer-modified binders with a softening point difference of less than 2.5 °C are considered thermal stable. Hence, 3% and 4% nanoclay stabilised HDPE-modified bituminous binder meets the specified criteria, indicating good storage stability.
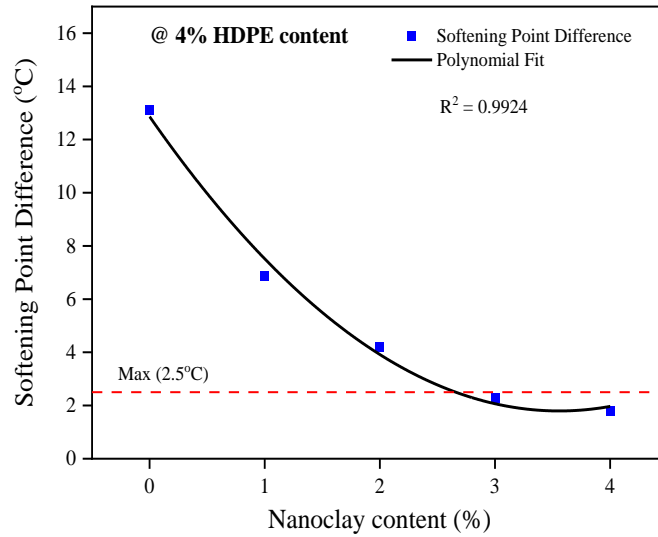
Fig. 9 Storage stability properties of HDPE-nanoclay stabilised binder

3.4.4. Marshall Stability and Flow Evaluation

As depicted in Fig. **10**a, incorporating 1%, 2%, and 3% nanoclay in 4%HDPE-modified mixture shows a stability increase of 10.8%, 16.5% and 30.2%, respectively. Although this trend was observed for all the content of nanoclay blends, the increment was more for the 4% HDPE-3% nanoclay blend. This enhancement is ascribed partially to the enhanced adhesion between aggregates and binders and partly to the likely increase in inter-particle friction induced by nanoclay particles. This improved adhesion and compatibility may have enhanced the mixture's workability, contributing to increased stability. On the other hand, incorporating 1%, 2%, 3%, and 4% NC particles reduces flow. As shown in Fig. **10**b, the flow of 1%, 2%, 3%, and 4% nanoclay decreases by 2.6%, 7.7%, 10.3% and 15.4%, respectively. The addition of nanoclay improves the adhesion of the bitumen binder with the aggregate. This increased adhesion can limit the flow of the bituminous mixture under load.
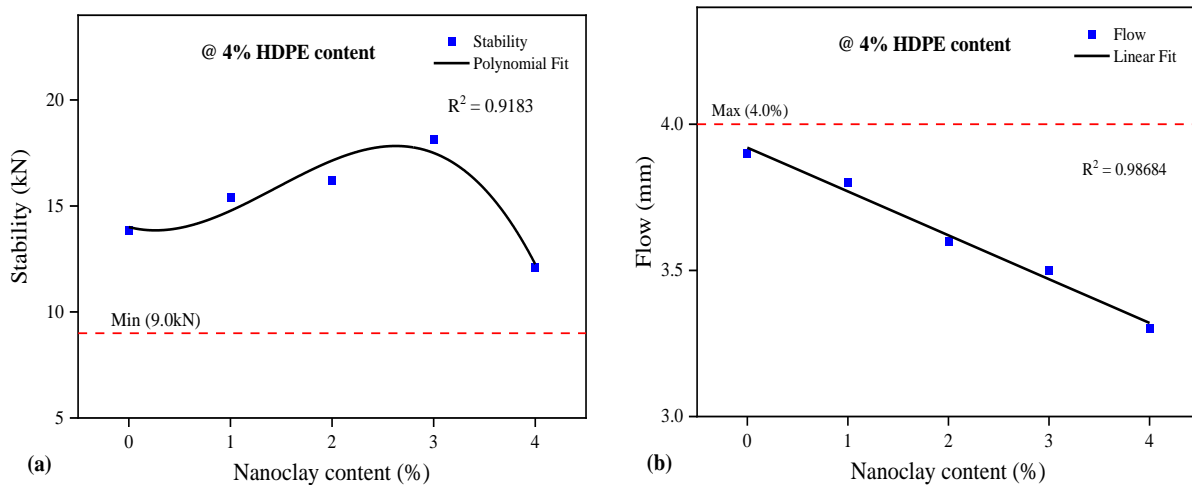

Fig. 10 Marshall properties of HDPE-nanoclay stabilised bituminous mixture (a) Stability, and (b) Flow.

3.4.5. Volumetric Properties

The results of VIM, VMA, and VFB of the HDPE-nanoclay modified bituminous mixture are depicted in Fig. 11a, b and c, respectively. It was observed that adding nanoclay reduced the air void and increased the VFB and VMA compared to the 4%HDPE-0%nanoclay modified bituminous mixture. An increase of 2.6%, 5.4%, 9.1% and 0.5% was recorded for VFB when incorporating 1%, 2%, 3% and 4% nanoclay, respectively. A reduction in air voids of 2.0%, 6.1%, and 12.3% was observed when 1%, 2% and 3% nanoclay were added, respectively.

The increase in VFB and reduction in VIM is ascribed to the nanostructure of clay particles, which enables them to fill the voids between the coated aggregates. Moreover, Fig. 11b shows that VMA increased with HDPE concentration. An increase of 0.7%, 2.8%, 7.1% and 10.6% was observed for 1, 2, 3, and 4% nanoclay dosage, respectively, compared to the HDPE-modified bitumen.

This may be attributed to the finesses and increased surface area of the nanoclay particles, which form a thick film around the aggregates. In comparison to the Kenya RDMIII specifications, as shown in Fig. 11, the HDPE-nanoclay bitumen mixture's air void, VMA, and VFB values meet AC binder course Type I specifications.

3.4.6. Microstructural Properties of High-Density Polyethylene-nanoclay Stabilised Binder

SEM images show the morphology and particle distribution of HDPE and nanoclay in the base and modified binder, respectively. EDS graphs show the binder's elementary composition. Fig. 12b indicates that as HDPE molecules interact with the base bitumen binder, the surface becomes smooth and shows a decreased appearance of the maltene component. Moreover, the addition of nanoclay, as depicted in Fig. 12 (c), (d), (e) and (f), shows that 1% nanoclay initiated interpenetration into the HDPE-modified binder, and 2% nanoclay caused the nanoclay particles to agglomerate. Furthermore, the addition of 3% and 4% nanoclay resulted in a clear dispersion of nanoclay in the phase of the HDPE-modified bituminous binder, indicating effective intercalation. This finding supported the improvement of phase separation when nanoclay was added. Analysis of the EDX results, as depicted in Figure 13, shows that the unmodified and HDPE-modified binders comprise carbon (C) and sulphur (S), indicating no new chemical element when HDPE is added. When 2%, 3%, and 4% nanoclay were added, silicon (Si) and oxygen (O) were added. Carbon and sulphur are associated mainly with HDPE-modified binder, whereas silicon and oxygen are related to nanoclay. The addition is due to the inorganic composition of the nanoclay
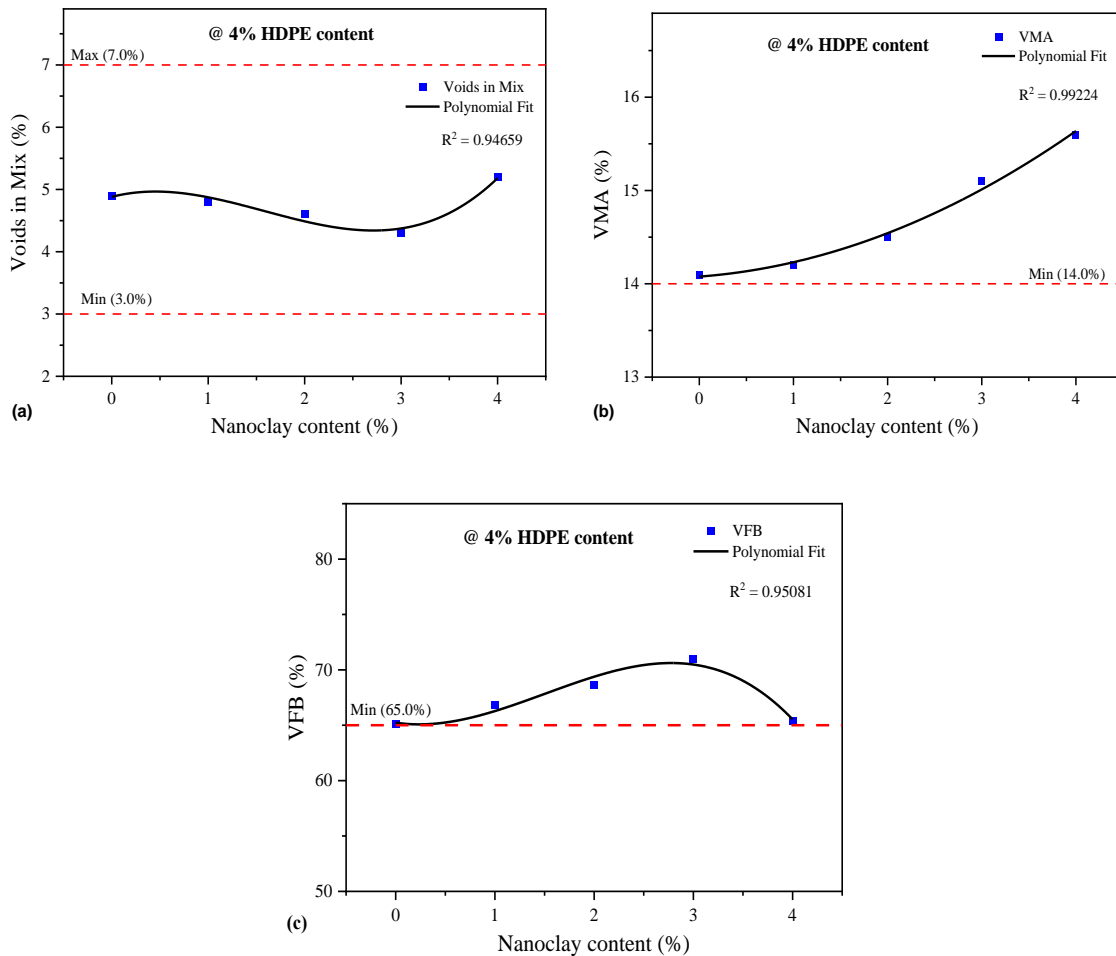

Fig. 11 Volumetric properties of HDPE-nanoclay stabilised bituminous mixture (a) Voids in mix (VIM), (b) Voids in mineral aggregates (VMA), and (c) voids filled with binder (VFB).
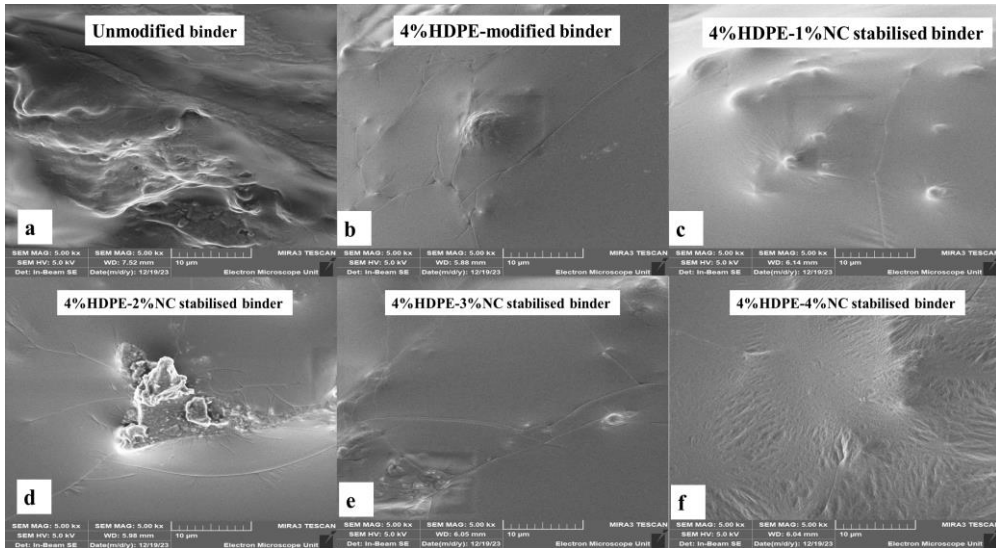
Fig. 12 Scanning electron microscopy micrograph of unmodified, HDPE-modified and HDPE-nanoclay stabilised binders
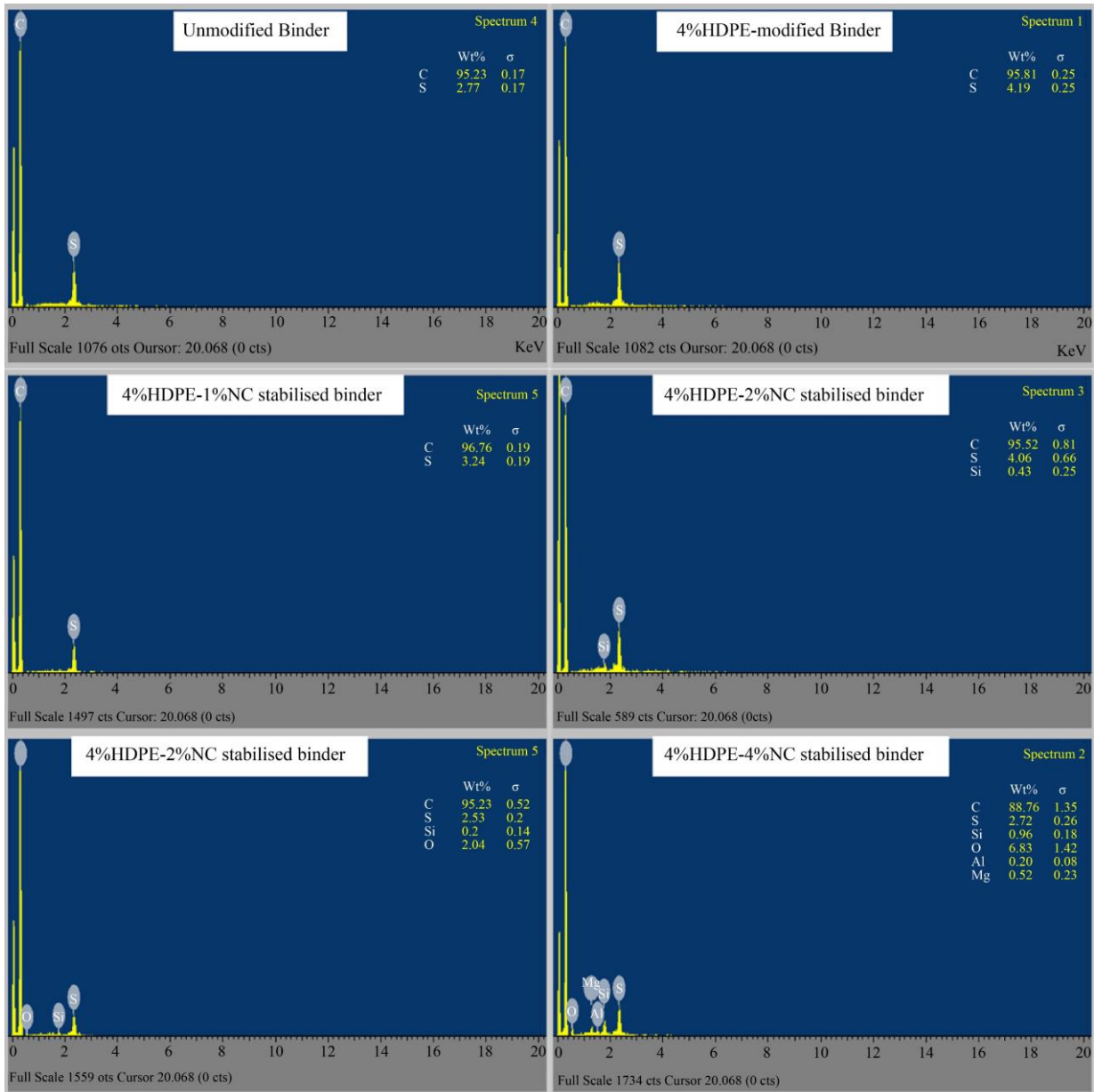

Fig. 13 Energy Dispersive X-ray Spectroscopy graph of unmodified, HDPE-modified and HDPE-nanoclay stabilised binders

The infrared spectra of unmodified, 4%HDPE-modified, and HDPE-NC stabilised bitumen binders are presented in Fig. **14**. The adsorption peaks at around 2928 cm^{-1} correspond to the asymmetric stretching vibration absorption peak of CH_2 (aliphatic hydrogen), and 2851 cm^{-1} is the symmetric stretching vibration absorption peak of CH_2 (aliphatic). The peak at around 1605 cm^{-1} is attributed to C=C stretch aromatics. Also, C–H bend alkanes and C-H symmetric bending of CH3 from bitumen were generated at 1462 cm^{-1} and 1374 cm^{-1}, respectively. The addition of 4%HDPE in the base binder shows a similar spectrum diagram with no apparent new peak in the spectrums. This indicates that 4%HDPE does not chemically react with the unmodified bitumen binder. However, a variation in the peak intensity of the unmodified bitumen binder was observed, indicating physical interaction between the HDPE and binder.

No new peaks appeared in the HDPE-nanoclay stabilised bitumen binder. However, the peak intensities decreased compared to the 4%HDPE-modified bitumen binder. This indicates a further physical interaction between HDPE-modified binder and nanoclay. This forms an interpenetrating network with the base binder, as the SEM images show.
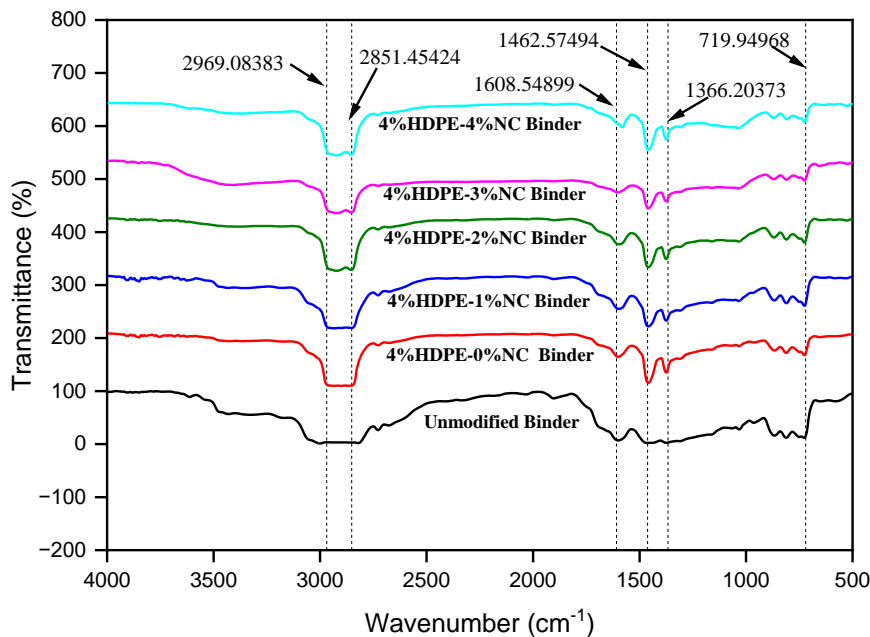

Fig. 14 Fourier Transform Infrared Spectroscopy plots of unmodified, HDPE-modified, and HDPE-nanoclay stabilised binders

4. Conclusion

This research evaluated the physical, rheological, volumetric, and Marshall properties of HDPE-modified binders incorporating nanoclay as stabilisers. The following conclusions are drawn from the findings.

1. The addition of the HDPE modifier increased the rutting resistance. Moreover, modified binders exhibited higher stiffness with increased viscosity.
2. The specimens prepared with the 4% HDPE recorded the highest stability, the lowest air voids, and the highest VFB. A stability increase indicates that the HDPE-modified mixes are much stronger than the control mix. Incorporating 6% and 8% of HDPE resulted in a decrease in stability and an increase in air voids. Compared with the specifications of the Kenya Design Manual for Roads and Bridges Part III, the most satisfactory performance was attained when 4% HDPE was incorporated.
3. Since HDPE does not have enough stability in bitumen binder during high-temperature storage, it can be stated that adding nanoclay improved HDPE-modified binder compatibility by enhancing its storage stability.
4. Incorporating nanoclay in HDPE-modified binder enhances rutting resistance and reduced workability.
5. The increased surface area of nanoclay may significantly improve the aggregate and binder adhesion, thus increasing Marshall stability and reducing air voids and flow of the HDPE-modified mix.
6. The SEM and FTIR results showed that 3% and 4% nanoclay yielded the most effective blending with HDPE-modified binder, indicating a successful penetration of nanoclay.
7. Compared with the Kenya Design Manual for Roads and Bridges Part III specifications, the 4% HDPE - 3%NC bitumen mix performed the best.
8. When comparing the 4% HDPE -3%NC bituminous mixture with the conventional bituminous mixture, Marshall stability increased by 48.4%, VFB increased by 7.3%, and air voids reduced by 12.2%. This indicated an improvement in strength and durability parameters.
9. The rutting resistance of 4% HDPE-3%NC bituminous binder is higher than that of the conventional binder for all testing temperatures. At 64°C, the rutting resistance was improved by 244.0%.

Acknowledgement

References

[1] Paolino Caputo et al., "Bitumen and Asphalt Concrete Modified by Nanometer-Sized Particles: Basic Concepts, the State of the Art and Future Perspectives of the Nanoscale Approach," *Advances in Colloid and Interface Science*, vol. 285, 2020. [CrossRef] [Google Scholar] [Publisher Link]

[2] Ramu Penki, and Subrat Kumar Rout, "Next-Generation Bitumen: A Review on Challenges and Recent Developments in Bio-Bitumen Preparation and Usage," *Biomass Conversion and Biorefinery*, vol. 13, pp. 9583-9600, 2023. [CrossRef] [Google Scholar] [Publisher Link]

[3] Yunus Erkuş, Baha Vural Kök, and Mehmet Yilmaz, "Evaluation of Performance and Productivity of Bitumen Modified by Three Different Additives," *Construction and Building Materials*, vol. 261, 2020. [CrossRef] [Google Scholar] [Publisher Link].

[4] Ana Dias et al., "Low-Temperature Performance of Polymer-Modified Binders in Stone Mastic Asphalts," *Infrastructures*, vol. 6, no. 4, pp. 1-22, 2021. [CrossRef] [Google Scholar] [Publisher Link]

[5] Jiqing Zhu, Björn Birgisson, and Niki Kringos, "Polymer Modification of Bitumen: Advances and Challenges," *European Polymer Journal*, vol. 54, pp. 18-38, 2014. [CrossRef] [Google Scholar] [Publisher Link]

[6] Sabzoi Nizamuddin, Yeong Jia Boom, and Filippo Giustozzi, "Sustainable Polymers from Recycled Waste Plastics and their Virgin Counterparts as Bitumen Modifiers: A Comprehensive Review," *Polymers*, vol. 13, no. 19, pp. 1-51, 2021. [CrossRef] [Google Scholar] [Publisher Link]

[7] Yuetan Ma et al., "The Utilization of Waste Plastics in Asphalt Pavements: A Review," *Cleaner Materials*, vol. 2, 2021. [CrossRef] [Google Scholar] [Publisher Link]

[8] Usman Ghani et al., "Comprehensive Study on the Performance of Waste HDPE and LDPE Modified Asphalt Binders for Construction of Asphalt Pavements Application," *Polymers*, vol. 14, no. 17, pp. 1-15, 2022. [CrossRef] [Google Scholar] [Publisher Link]

[9] Fereidoon Moghadas Nejad, Alireza Azarhoosh, and Gholam Hossein Hamedi, "Effect of High-Density Polyethylene on the Fatigue and Rutting Performance of Hot Mix Asphalt – A Laboratory Study," *Road Materials and Pavement Design*, vol. 15, no. 3, pp. 746-756, 2014. [CrossRef] [Google Scholar] [Publisher Link]

[10] Elizabeth Langa et al., "Effect of Vegetable Oil on the Properties of Asphalt Binder Modified with sHigh-Density Polyethylene," *Polymers*, vol. 15, no. 3, pp. 1-15, 2023. [CrossRef] [Google Scholar] [Publisher Link]

[11] Behnam Golestani et al., "Nanoclay Application to Asphalt Concrete: Characterization of Polymer and Linear Nanocomposite-Modified Asphalt Binder and Mixture," *Construction and Building Materials*, vol. 91, pp. 32-38, 2015. [CrossRef] [Google Scholar] [Publisher Link]

[12] Ahmad Mansourian, Ali Rezazad Goahri, and Fariba Karimian Khosrowshahi, "Performance Evaluation of Asphalt Binder Modified with EVA/HDPE/Nanoclay Based on Linear and Non-Linear Viscoelastic Behaviors," *Construction and Building Materials*, vol. 208, pp. 554-563, 2019. [CrossRef] [Google Scholar] [Publisher Link]

[13] Zhen Leng et al., "Improvement of Storage Stability of SBS-Modified Asphalt with Nanoclay Using a New Mixing Method," *Road Materials and Pavement Design*, vol. 20, no. 7, pp. 1601-1614, 2019. [CrossRef] [Google Scholar] [Publisher Link]

[14] Mohd Ezree Abdullah et al., "Engineering Properties of Asphalt Binders Containing Nanoclay and Chemical Warm-Mix Asphalt Additives," *Construction and Building Materials*, vol. 112, pp. 232-240, 2016. [CrossRef] [Google Scholar] [Publisher Link]

[15] Mahmoud Ameri et al., "Investigating Effects of Nano/SBR Polymer on Rutting Performance of Binder and Asphalt Mixture," *Advances in Materials Science and Engineering*, vol. 2018, pp. 1-8, 2018. [CrossRef] [Google Scholar] [Publisher Link]

[16] Behrooz Sedaghat et al., "Rheological Properties of Bitumen Containing Nanoclay and Organic Warm-Mix Asphalt Additives," *Construction and Building Materials*, vol. 243, 2020. [CrossRef] [Google Scholar] [Publisher Link]

[17] Zhibin Ren et al., "Enhanced Storage Stability of Different Polymer Modified Asphalt Binders through Nano-Montmorillonite Modification," *Nanomaterials*, vol. 10, no. 4, pp. 1-17, 2020. [CrossRef] [Google Scholar] [Publisher Link]

[18] Ashraf Abdel-Raheem et al., "Investigating the Potential of High-Density Polyethylene and Nano Clay Asphalt-Modified Binders to Enhance the Rutting Resistance of Asphalt Mixture," *Sustainability*, vol. 15, no. 18, pp. 1-19, 2023. [CrossRef] [Google Scholar] [Publisher Link]

[19] ASTM D36-06, Standard Test Method for Softening Point of Bitumen (Ring-and-Ball Apparatus), ASTM International Standards Organization, pp. 1-4, 2010. [CrossRef] [Publisher Link]

[20] ASTM D113, Standard Test Method for Ductility of Asphalt Materials, ASTM International Standards Organization, pp. 1-5, 2017. [CrossRef] [Google Scholar] [Publisher Link]

[21] ASTM D5-05, Standard Test Method for Penetration of Bituminous Materials, ASTM International Standards Organization, pp. 1-4, 2013. [CrossRef] [Google Scholar] [Publisher Link]

[22] AASHTO T316-22, "*Standard Method of Test for Viscosity Determination of Asphalt Binder Using Rotational Viscometer*," American Association of State and Highway Transportation Officials, 2022. [Google Scholar] [Publisher Link]

[23] Eyad Masad et al., "*A Review of Asphalt Modification Using Plastics: A Focus on Polyethylene*," Texas A&M University at Qatar, Doha, pp.1-26, 2020. [Google Scholar]

[24] AASHTO Designation: T 315-12, "*Standard Method of Test for: Determining the Rheological Properties of Asphalt Binder Using a Dynamic Shear Rheometer (DSR)*," American Association of State Highway and Transportation Officials, 2011. [Google Scholar] [Publisher Link]

[25] ASTM D7173-20, Standard Practice for Determining the Separation Tendency of Polymer from Polymer Modified Asphalt, ASTM International Standards Organization, pp. 1-2, 2005. [CrossRef] [Google Scholar] [Publisher Link]

[26] ASTM D1559-89, Test Method for Resistance to Plastic Flow of Bituminous Mixtures Using Marshall Apparatus, ASTM International Standards Organization, 1989. [Google Scholar] [Publisher Link]

[27] ASTM D6927-22, Standard Test Method for Marshall Stability and Flow of Asphalt Mixtures, ASTM International Standards Organization, pp. 1-7, 2022. [CrossRef] [Google Scholar] [Publisher Link]

[28] Sileola B. Ogunlaja, and Rajinder Pal, "Effects of Bentonite Nanoclay and Cetyltrimethyl Ammonium Bromide Modified Bentonite Nanoclay on Phase Inversion of Water-in-Oil Emulsions," *Colloids and Interfaces*, vol. 4, no. 1, pp. 1-14, 2020. [CrossRef] [Google Scholar] [Publisher Link]